

# Thermal analysis and Infrared emission spectroscopic study of kaolinite–potassium acetate intercalate complex

Hongfei Cheng · Jing Yang · Ray L. Frost ·  
Qinfu Liu · Zhiliang Zhang

Received: 21 April 2010 / Accepted: 3 June 2010 / Published online: 17 June 2010  
© Akadémiai Kiadó, Budapest, Hungary 2010

**Abstract** The thermal behavior and decomposition of kaolinite–potassium acetate intercalation complex was investigated through a combination of thermogravimetric analysis and infrared emission spectroscopy. Three main changes were observed at 48, 280, 323, and 460 °C which were attributed to (a) the loss of adsorbed water, (b) loss of the water coordinated to acetate ion in the layer of kaolinite, (c) loss of potassium acetate in the complex, and (d) water through dehydroxylation. It is proposed that the potassium acetate intercalation complex is stability except heating at above 300 °C. The infrared emission spectra clearly show the decomposition and dehydroxylation of the kaolinite intercalation complex when the temperature is raised. The dehydration of the intercalation complex is followed by the loss of intensity of the stretching vibration bands at region 3600–3200  $\text{cm}^{-1}$ . Dehydroxylation is followed by the decrease in intensity in the bands between 3695 and 3620  $\text{cm}^{-1}$ . Dehydration is completed by 400 °C and partial dehydroxylation by 650 °C. The inner hydroxyl group remained until around 700 °C.

**Keywords** Kaolinite · Potassium acetate · Intercalation complex · Infrared emission spectroscopy

H. Cheng  
School of Mining Engineering, Inner Mongolia University of Science and Technology, Baotou 014010, China

H. Cheng · J. Yang · R. L. Frost (✉)  
Chemistry Discipline, Faculty of Science and Technology,  
Queensland University of Technology, 2 George Street,  
GPO Box 2434, Brisbane, QLD 4001, Australia  
e-mail: r.frost@qut.edu.au

H. Cheng · Q. Liu · Z. Zhang  
School of Geoscience and Surveying Engineering, China  
University of Mining and Technology, Beijing 100083, China

## Introduction

Kaolinite has been and continues to be one of the most important and useful industrial minerals. It is widely applied in the fabrication of paper, paints and inks, rubber and plastic, ceramic raw material, fiberglass, cracking catalysts, cosmetics, medicines, etc. [1–3]. Recent advances in the preparation of hybrid organic–inorganic materials by intercalation of organic molecules into kaolinite represent a clear possibility of new and interesting materials [4]. Kaolinite can interact with organic molecules by intercalation which is a process of insertion of molecules between the kaolinite layers. This process involves the breaking of hydrogen bonds between the kaolinite layers and the formation of new hydrogen bonds with the inserting molecule [5].

Therefore, an important part of research in laboratory is focused on the preparation of the complexes of kaolinite intercalated by organic molecules. This area, essentially making the clay into a single-layered mineral, has gained much attention over recent decades. The inserting molecule breaks the hydrogen bonds formed between the kaolinite hydroxyl groups and the oxygen of the next adjacent siloxane layer, then forms hydrogen bonds with either the hydrophobic surface of the kaolinite (the siloxane layer) or the hydrophilic part of the kaolinite surface (the hydroxyl surfaces of the gibbsite-like layer). A further possibility exists in that the inserting or adsorbing molecule may interact with the surfaces of the kaolinite [6, 7]. The kaolinite intercalated with reactive guest molecules can also be used as precursors for the intercalation of nonreactive organic molecules via the displacement of intercalated molecules. In addition to the formation of new organoclay nanohybrid materials, intercalation can lead to the covalent grafting of organic molecules. Therefore,

kaolinite-potassium acetate intercalation complex has the potential to be a precursor for polymer-kaolinite intercalation complexes [8].

There have been a significant number of preparation routes of kaolinite intercalation complex [9–13]. Recently, some new methods for intercalation of kaolinite have been reported, in which the layered kaolinite particles were intercalated with small molecules, such as urea, potassium acetate, dimethylsulfoxide, and so on. These inserting molecules expand the interlayer space of kaolinite, allowing the interlayer hydroxyl group to be accessed by organic molecules [14–16].

Regardless of the extensive use of kaolinite in industrial processes and its excellent characteristics for the preparation of organic/inorganic intercalation complexes, there is little information about the thermal stability of intercalation complex. However, heating treatment of intercalated kaolinite is necessary for its further application, especially in the field of plastic and rubber industry. Infrared emission spectroscopy allows the possibility of studying the decomposition, dehydration, and dehydroxylation of kaolinite intercalation complex at elevated temperatures. This technique of measurement of discrete vibrational frequencies emitted by thermally excited molecules, known as Fourier transform infrared emission spectroscopy (FT-IES), has not been widely used for study of thermal stability of clay intercalation complex [17–20]. In this study, thermogravimetric analysis and infrared emission spectroscopy were used to investigate the changes in the complex of kaolinite intercalated by potassium acetate.

## Experimental methods

### Materials

The sample used in this study was the natural pure kaolinite from Hebei Zhangjiakou in China. Its chemical composition in wt% is SiO<sub>2</sub> 44.64, Al<sub>2</sub>O<sub>3</sub> 38.05, Fe<sub>2</sub>O<sub>3</sub> 0.22, MgO 0.06, CaO 0.11, Na<sub>2</sub>O 0.27, K<sub>2</sub>O 0.08, TiO<sub>2</sub> 1.13, P<sub>2</sub>O<sub>5</sub> 0.13, MnO 0.002, LOT (loss on ignition) 15.06. The major mineral constituent is well-ordered kaolinite (95 wt%) with a Hinckley index of 1.31. The potassium acetate (A. R) was purchased from Beijing Chemical Reagents Company, China.

### The intercalation composite preparation

The potassium acetate (KAc) intercalate complex was prepared by immersing 10 g of kaolinite in 20 ml of KAc solution at a mass percentage concentration of 30%, stirring for 10 min at room temperature. The complex after aging for 24 h was allowed to dry at room temperature

before the X-ray diffraction (XRD), thermogravimetric analysis (TG), and Infrared emission spectroscopy (IES).

### X-ray diffraction

X-ray diffraction patterns were collected using a PANalytical X'Pert PRO X-ray diffractometer (radius: 240.0 mm). Incident X-ray radiation was produced from a line focused PW3373/10 Cu X-ray tube, operating at 40 kV and 40 mA, with Cu K $\alpha$  radiation of 1.540596 Å. The incident beam passed through a 0.04 rad soller slit, a 1/2° divergence slit, a 15 mm fixed mask, and a 1° fixed anti-scatter slit.

### Thermogravimetric analysis (TG)

Thermogravimetric analysis (TG) of the sample was carried out in a TA<sup>®</sup> Instruments incorporated high-resolution thermo gravimetric analyzer (series Q500) in a flowing nitrogen atmosphere (60 cm<sup>3</sup> min<sup>-1</sup>). Approximately 50 mg of each sample underwent thermal analysis, with a heating rate of 5 °C/min, with resolution of 6, from room temperature to 1000 °C.

### Infrared emission spectroscopy

FTIR emission spectroscopy was carried out on a Nicolet Nexus 870 FTIR spectrometer, which was modified by replacing the IR source with an emission cell. A description of the cell and principles of the emission experiment have been published elsewhere [17–19, 21]. Approximately 0.2 mg of kaolinite-potassium acetate intercalation complex was spread as a thin layer on a 6 mm diameter platinum surface and held in an inert atmosphere within a nitrogen-purged cell during heating. The infrared emission cell consists of a modified atomic absorption graphite rod furnace, which is driven by a thyristor-controlled AC power supply capable of delivering up to 150 A at 12 V. A platinum disk acts as a hot plate to heat the kaolinite intercalation complex sample and is placed on the graphite rod. An insulated 125  $\mu$ m type R thermocouple was embedded inside the platinum plate in such a way that the thermocouple junction was less than 0.2 mm below the surface of the platinum. Temperature control of  $\pm 2$  °C at the operating temperature of the sample was achieved by using a Eurotherm Model 808 proportional temperature controller, coupled to the thermocouple.

In the normal course of events, three sets of spectra are obtained over the temperature range selected and at the same temperatures; those of the black body radiation, the platinum plate radiation, and the platinum plate covered with the sample. Normally only one set of black body and platinum radiation is required. The emission spectrum at a

particular temperature was calculated by subtraction of the single beam spectrum of the platinum backplate from that of the platinum covered with the sample, and the result ratioed to the single beam spectrum of an approximate black body (graphite). This spectral manipulation is carried out after all the spectral data have been collected.

The emission spectra were collected at intervals of 50 °C over the range 100–1000 °C. The time between scans (while the temperature was raised to the next hold point) was approximately 100 s. It was considered that this was sufficient time for the heating block and the powdered sample to reach temperature equilibrium. The spectra were acquired by co-addition of 128 scans for the whole temperature range, with an approximate scanning time of 1 min, and a nominal resolution of 4 cm<sup>-1</sup>. Good quality spectra can be obtained providing the sample thickness is not too large. If too large a sample is used then the spectra become difficult to interpret due to the presence of combination and overtone bands. Spectral manipulation such as baseline adjustment, smoothing, and normalization was performed using the Spectra calc software package (Galactic Industries Corporation, NH, USA).

## Results and discussion

### X-ray diffraction (XRD)

X-ray diffraction is the preliminary technique to verify whether the layered structure is altered or not [22]. When the kaolinite was intercalated with KAc solution, expansion occurred along the C-axis only [23]. Figure 1 shows the XRD patterns of kaolinite and its intercalated complex with KAc. The XRD pattern shows that the basal  $d_{(001)}$  of kaolinite expands from 0.718 to 1.425 nm; this value is indicative of the intercalation of KAc in the interlamellar space of kaolinite, and which is consistent with the results published before [5, 24, 25]. Kaolinite shows an identical XRD pattern to the standard and a characteristic first basal peak at 0.718 nm, which decrease in intensity when intercalated by KAc.

### Thermal analysis

Thermal analysis can reveal information about the thermal decomposition of intercalated kaolinite [26]. To evaluate the thermal stability of kaolinite–KAc intercalation complex, the thermogravimetric and differential thermogravimetric (TG-DTG) measurement of kaolinite and kaolinite–KAc intercalation complex were performed and results are shown in Fig. 2a,b. Only one mass loss is observed in the TG-DTG curves of kaolinite in Fig. 2a at 464 °C with mass loss of 13.65%, which is attributed to the dehydroxylation of

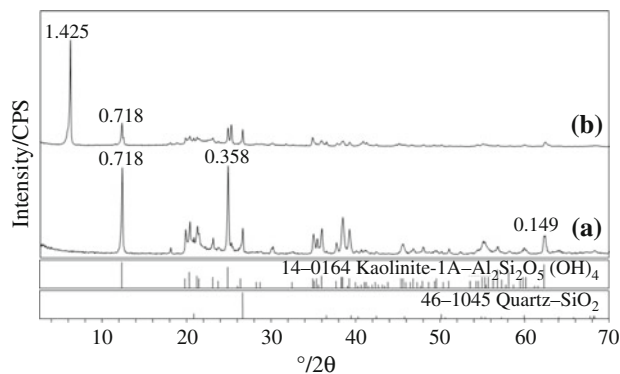


**Fig. 1** The XRD patterns for **a** kaolinite, **b** kaolinite–KAc intercalation complex

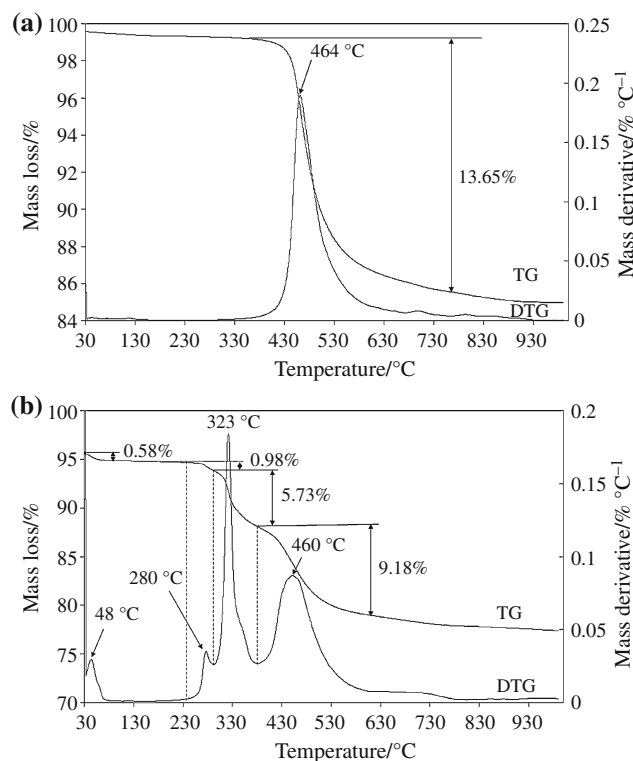


**Fig. 2** Thermal analysis curves (TG-DTG) of **a** kaolinite and **b** kaolinite–KAc intercalation complex

kaolinite. This value was close to the theoretical value (13.9%). However, four distinct mass losses are observed in the TG-DTG curves of kaolinite–KAc intercalation complex in Fig. 2b. The TG-DTG curve of the intercalation complex presented a peak at 48 °C associated with dehydration of the material with a 0.58% mass loss of physisorbed water. The second peak appeared at 280 °C, accompanied by a mass loss of 0.98% caused by decomposition of the intercalation complex. It is well known that the kaolinite–KAc intercalation complex was formed from the expansion of kaolinite with both KAc and water molecular [5, 12]. This step can be interpreted as being due to the loss of intercalated water

which is coordinated to KAc in the interlayer of kaolinite. Figure 2b also shows another peak at 323 °C assigned to the loss of KAc in the layer of intercalation complex. The last mass loss of 9.18% at 460 °C is observed, which is attributed to the dehydroxylation of kaolinite.

The results similar to the aforementioned observations were previously found [26]. It is generally considered that a set of steps are there for the dehydration, loss of KAc, and dehydroxylation of the intercalation complex. These steps correspond to (a) the loss of adsorbed water, (b) the loss of coordination water, (c) the loss of KAc, and (d) water through dehydroxylation.

### Infrared emission spectroscopy

The infrared emission spectra of kaolinite–KAc intercalation complex show considerable complexity. Figure 3 shows the infrared emission spectra of kaolinite–KAc intercalation complex. The spectra clearly show the temperature at which the OH group is lost and at which the complex decomposed. In the 200–600 °C temperature range obvious structure changes are observed. In order to follow these thermal decompositions three spectra at 200, 400, and 600 °C were selected for further analysis. The infrared emission spectra at these temperatures for kaolinite–KAc intercalation complex in the 650–1350  $\text{cm}^{-1}$

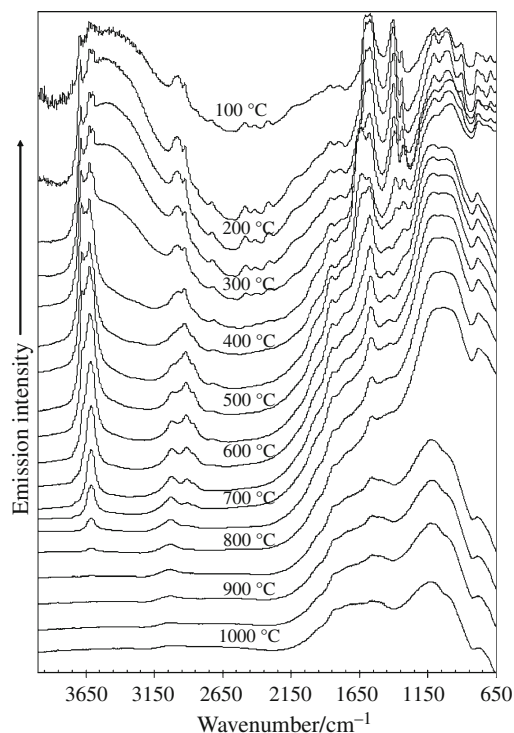


**Fig. 3** Infrared emission spectra of kaolinite–KAc intercalation complex over the 100–1000 °C temperature range

range are shown in Fig. 4. At 200 °C, the spectrum in this region presents two bands at 754 and 790  $\text{cm}^{-1}$ , which are typical of the OH translational vibrations. The bands at 914 and 937  $\text{cm}^{-1}$  are attributed to the OH bending vibrations. Two strong bands at 983 and 1035  $\text{cm}^{-1}$  are assigned to the Si–O–Si in-plane vibrations. The band occurring at 1115  $\text{cm}^{-1}$  is the Si–O stretching mode. The band is observed at 1157  $\text{cm}^{-1}$ . One probable assignment of this band is to the stretching mode of Si–O from quartz impurity. The 400 °C spectrum shows small shift in these bands, which are now observed at 725, 783, 980, 1038, 1150, 1201  $\text{cm}^{-1}$ . Four bands at 694, 800, 914, and 937  $\text{cm}^{-1}$  disappeared, and a new band is observed at 1201  $\text{cm}^{-1}$ . These shift and disappearance are attributed to that the water coordinated to KAc is lost when the temperature is raised. These also illustrate that when KAc is actually intercalated into the layer of kaolinite and attached with the inner surface hydroxyl of kaolinite it will result in the shift of Al–O. These bands are observed at 725, 785, 935, 998, and 1142  $\text{cm}^{-1}$  in the 600 °C spectrum.

The infrared emission spectra of kaolinite–KAc intercalation complex at 200, 400, and 600 °C in the 1250–1750  $\text{cm}^{-1}$  range are shown in Fig. 5. Infrared bands in this spectral region are associated with the KAc vibrations modes. The symmetric stretching band of the O–C–O unit in KAc shifted to 1403  $\text{cm}^{-1}$  as a result of hydrogen bonding with inner surface OH groups in the complex. At

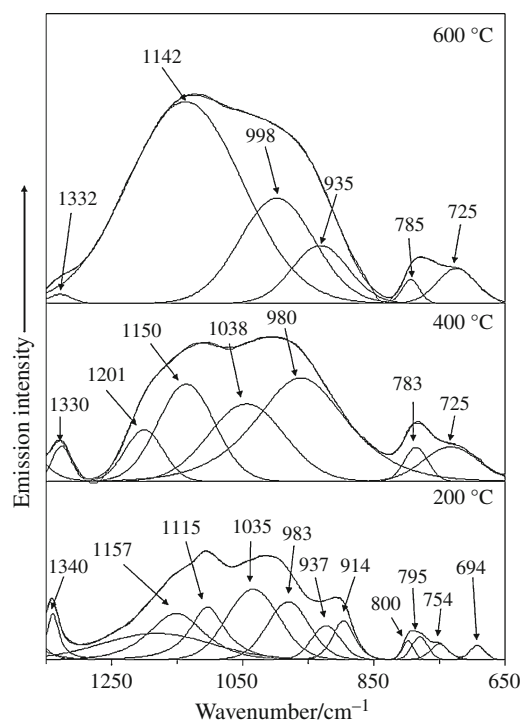


**Fig. 4** Infrared emission spectra of kaolinite–KAc intercalation complex in the 650–1300  $\text{cm}^{-1}$  region at 200, 400, and 600 °C

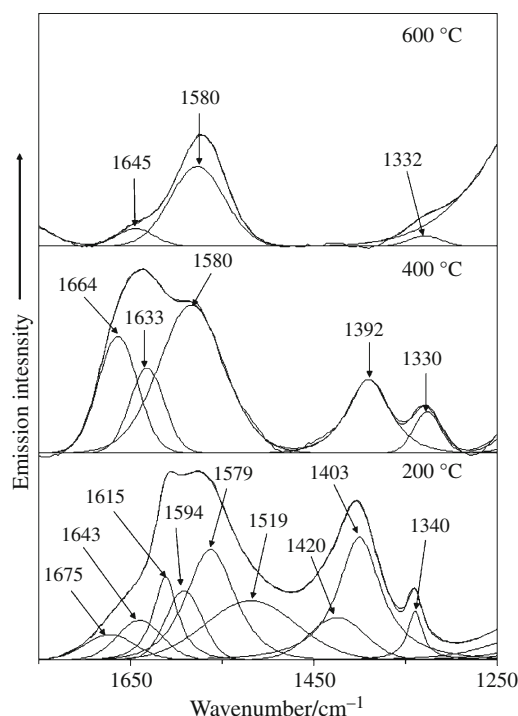


**Fig. 5** Infrared emission spectra of kaolinite–KAc intercalation complex in the 1250–1750  $\text{cm}^{-1}$  region at 200, 400, and 600  $^{\circ}\text{C}$

the same time, the symmetric deformation band of the  $\text{CH}_3$  group was reduced in intensity at 1340  $\text{cm}^{-1}$ . It is proposed that the  $\text{CH}_3$  group of the acetate is interacting with the silica sheet [8]. The bands are observed at 200  $^{\circ}\text{C}$  at 1579 and 1420  $\text{cm}^{-1}$ , which are due to the antisymmetric and symmetric  $\nu$  (COO) stretching vibrations. Two bands are observed at 1519 and 1594  $\text{cm}^{-1}$  are attributed to acetate ion antisymmetric stretching modes [17]. The band at 1643  $\text{cm}^{-1}$  is assigned to the water bending vibration. This band is not observed at 400  $^{\circ}\text{C}$  or above this temperature. Therefore, the water is lost below 400  $^{\circ}\text{C}$ , which is consistent with the thermal analysis data and the result before [26]. The band at 1675  $\text{cm}^{-1}$  is due to the C=O vibration. These bands are observed at 1330, 1392, 1580, 1633, and 1664  $\text{cm}^{-1}$  in the 400  $^{\circ}\text{C}$  spectrum. Only three bands are observed for this complex at 600  $^{\circ}\text{C}$ , at 1332, 1580, and 1645  $\text{cm}^{-1}$ . They are clearly shown the thermal decomposition of kaolinite–KAc intercalation complex when the temperature is raised.

Figure 6 illustrates the infrared emission spectra of the hydroxyl stretching bands of the kaolinite–KAc intercalation complex over the temperature range 200 to 600  $^{\circ}\text{C}$ . The figure clearly shows the loss of intensity of these bands as the temperature is raised. Considerable differences are observed between the relative intensity of the bands at 200  $^{\circ}\text{C}$  and 600  $^{\circ}\text{C}$ . The infrared emission spectra of kaolinite–KAc intercalation complex at 200  $^{\circ}\text{C}$  in the

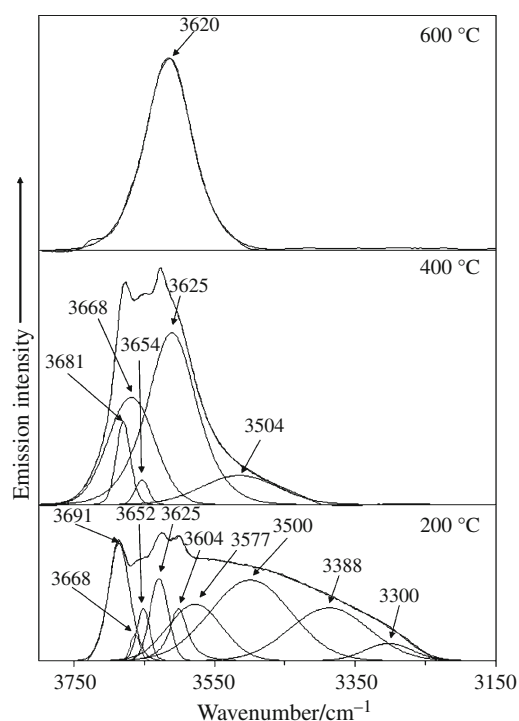


**Fig. 6** Infrared emission spectra of kaolinite–KAc intercalation complex in the 3150–3800  $\text{cm}^{-1}$  region at 200, 400, and 600  $^{\circ}\text{C}$

hydroxyl stretching region show important features [8, 11, 27–30]: bands are observed at (a) ( $\nu_1$ ) 3691  $\text{cm}^{-1}$ , which is attributed to the hydroxyl stretching of the inner surface hydroxyl (b) bands ( $\nu_2$ ) at 3668  $\text{cm}^{-1}$  assigned to the out-of-phase vibration of the inner surface hydroxyls (c) bands ( $\nu_3$ ) at 3652  $\text{cm}^{-1}$  attributed to the second out-of-phase vibration of the inner surface hydroxyls (d) bands ( $\nu_5$ ) at 3625  $\text{cm}^{-1}$  attributed to the inner hydroxyls (e) bands ( $\nu_6$ ) at 3604  $\text{cm}^{-1}$  attributed to formation of the hydrogen bonding of the inner surface hydroxyls and the acetate and (f) bands ( $\nu_{7-9}$ ) at 3577, 3500, 3388, and 3300  $\text{cm}^{-1}$  attributed to the hydroxyls stretching frequency of inter-layer water coordinated to KAc. In the 400  $^{\circ}\text{C}$  spectrum only five bands are observed at 3681, 3668, 3654, 3625, and 3504  $\text{cm}^{-1}$ . However, only one band is found at 3620  $\text{cm}^{-1}$  in the 600  $^{\circ}\text{C}$  spectrum. This means that the inner hydroxyl was not affected by intercalated KAc. This result consistent with the inner hydroxyls is below the aluminum atoms and extends toward the intralayer cavity (vacant octahedral site) of the kaolinite [31–33].

## Conclusions

The TG-DTG investigation of the intercalation complex enabled the thermal characteristics of the deintercalation of the KAc intercalated kaolinite to be obtained. A set of steps



for the dehydration were observed, which were attributed to (a) the loss of adsorbed water at 48 °C, (b) the loss of coordination water at 280 °C, and (c) water through dehydroxylation at 460 °C. It was also clearly shown the loss of KAc in the layer of intercalation complex at 323 °C. The thermal analysis data were used to select appropriate temperatures for the collection of infrared emission spectra data. The technique of infrared emission spectroscopy allows the possibility of studying intercalation of minerals such as kaolinite–KAc intercalation complex and to study the thermal decomposition of these minerals in situ at the elevated temperatures. The technique also helps confirm the assignment of various kind bands. Organoclay such as kaolinite–KAc intercalation complex and the thermal products of kaolinite have application as rubber and infrared emission spectroscopy enables the study of these materials for potential use as rubber and plastic. The decomposition of intercalation complex was confirmed by the infrared emission spectra which show the intercalation complex is stable up to around 300 °C.

**Acknowledgements** The authors gratefully acknowledge the financial support provided by the National “863” project of China (2008AA06Z109) and infra-structure support of the Queensland University of Technology Chemistry Discipline, Faculty of Science and Technology.

## References

1. Franco F, Pérez-Maqueda LA, Pérez-Rodríguez JL. The effect of ultrasound on the particle size and structural disorder of a well-ordered kaolinite. *J Colloid Interface Sci.* 2004;274:107–17.
2. Zhang X, Fan D, Xu Z. Rapid preparation for kaolinite/dimethyl sulphoxide intercalated complex induced by microwave. *J Tongji Univ (Natural Science).* 2005;33:1646–50.
3. Franco F, Cecilia JA, Pérez-Maqueda LA, Pérez-Rodríguez JL, Gomes CSF. Particle-size reduction of dickite by ultrasound treatments: effect on the structure, shape and particle-size distribution. *Appl Clay Sci.* 2007;35:119–27.
4. Gardolinski JE, Peralta-Zamora P, Wypych F. Preparation and characterization of a kaolinite-1-methyl-2-pyrrolidone intercalation compound. *J Colloid Interface Sci.* 1999;211:137–41.
5. Frost RL, Kristof J, Klopogge JT, Horvath E. Rehydration of potassium acetate-intercalated kaolinite at 298 K. *Langmuir.* 2000;16:5402–8.
6. Frost RL, Kristof J, Horvath E, Klopogge JT. Deintercalation of dimethylsulphoxide intercalated kaolinites—a DTA/TGA and Raman spectroscopic study. *Thermochim Acta.* 1999;327:155–66.
7. Frost RL, Kristof J, Horvath E, Klopogge JT. Modification of the kaolinite hydroxyl surfaces through the application of pressure and temperature. Part III. *J Colloid Interface Sci.* 1999;214:380–8.
8. Horváth E, Kristóf J, Frost RL. Vibrational spectroscopy of intercalated kaolinites. Part I. *Appl Spectrosc Rev.* 2010;45:130–47.
9. Gardolinski JEF, Lagaly G. Grafted organic derivatives of kaolinite: I. Synthesis, chemical and rheological characterization. *Clay Miner.* 2005;40:537–46.
10. Zhao S, Wang T, Xu H, Guo Y. Preparation of kaolinite/p-toluene sulfonic acid intercalation compound by melting method. *Feijinshukuang* 2009;32:37–9.
11. Frost RL, Kristof J, Paroz GN, Tran TH, Klopogge JT. The role of water in the intercalation of kaolinite with potassium acetate. *J Colloid Interface Sci.* 1998;204:227–36.
12. Koji W. Lattice expansion of kaolin minerals by treatment with potassium acetate. *Am Miner.* 1961;46:78–91.
13. Anakli D, Çetinkaya S. Preparation of poly(2-ethyl aniline)/kaolinite composite materials and investigation of their properties. *Curr Appl Phys.* 2010;10:401–6.
14. Janek M, Emmerich K, Heissler S, Nuesch R. Thermally induced grafting reactions of ethylene glycol and glycerol intercalates of kaolinite. *Chem Mater.* 2007;19:684–93.
15. Letaief S, Elbokl TA, Detellier C. Reactivity of ionic liquids with kaolinite: melt intercalation of ethyl pyridinium chloride in an urea-kaolinite pre-intercalate. *J Colloid Interface Sci.* 2006;302:254–8.
16. Letaief S, Detellier C. Interlayer grafting of glycidol (2, 3-epoxy-1-propanol) on kaolinite. *Can J Chem.* 2008;86:1–6.
17. Frost RL, Bahfenne S, Graham J. Infrared and infrared emission spectroscopic study of selected magnesium carbonate minerals containing ferric iron—Implications for the geosequestration of greenhouse gases. *Spectrochim Acta A Mol Biomol Spectrosc.* 2008;71:1610–6.
18. Frost RL, Klopogge JT. Infrared emission spectroscopic study of brucite. *Spectrochim Acta A Mol Biomol Spectrosc.* 1999;55:2195–205.
19. Frost RL, Weier ML. Thermal treatment of weddellite—a Raman and infrared emission spectroscopic study. *Thermochim Acta.* 2003;406:221–32.
20. Frost RL, Cash GA, Klopogge JT. ‘Rocky Mountain leather’, sepiolite and attapulgite—an infrared emission spectroscopic study. *Vib Spectrosc.* 1998;16:173–84.
21. Frost RL, Wain D. A thermogravimetric and infrared emission spectroscopic study of alunite. *J Therm Anal Calorim.* 2008;91:267–74.
22. Arizaga GGC, Gardolinski JEF, Schreiner WH, Wypych F. Intercalation of an oxalatoxonioate complex into layered double hydroxide and layered zinc hydroxide nitrate. *J Colloid Interface Sci.* 2009;330:352–8.
23. Zhang B, Li Y, Pan X, Jia X, Wang X. Intercalation of acrylic acid and sodium acrylate into kaolinite and their in situ polymerization. *J Phys Chem Solids.* 2007;68:135–42.
24. Franco F, Ruiz Cruz MD. Factors influencing the intercalation degree (‘reactivity’) of kaolin minerals with potassium acetate, formamide, dimethylsulphoxide and hydrazine. *Clay Miner.* 2004;39:193–205.
25. Frost RL, Kristof J, Horvath E, Klopogge JT. Modification of kaolinite surfaces through intercalation with potassium acetate, II. *J Colloid Interface Sci.* 1999;214:109–17.
26. Cheng H, Liu Q, Yang J, Zhang Q, Frost RL. Thermal behavior and decomposition of kaolinite-potassium acetate intercalation composite. *Thermochim Acta.* 2010;503–504:16–20.
27. Frost RL, Kristof J, Horvath E, Klopogge JT. Effect of water on the formamide-intercalation of kaolinite. *Spectrochim Acta A Mol Biomol Spectrosc.* 2000;56:1711–29.
28. Frost RL, Kristof J, Mako E, Horvath E. A DRIFT spectroscopic study of potassium acetate intercalated mechanochemically activated kaolinite. *Spectrochim Acta A Mol Biomol Spectrosc.* 2003;59:1183–94.
29. Frost RL, Kristof J, Paroz GN, Klopogge JT. Role of water in the intercalation of kaolinite with hydrazine. *J Colloid Interface Sci.* 1998;208:216–25.
30. Franco F, Ruiz Cruz M. Thermal behaviour of dickite-dimethylsulfoxide intercalation complex. *J Therm Anal Calorim.* 2003;73:151–65.
31. Gorb LG, Aksechenko EV, Adams JW, Larson SL, Weiss CA, Leszczynska D, Leszczynski J. Computational design of clay

- minerals: hydration of Mg-exchange cation located in ditrigonal cavity. *J Mol Struct.* 1998;425:129–35.
32. Hess AC, Saunders VR. Periodic ab initio Hartree-Fock calculations of the low-symmetry mineral kaolinite. *J Phys Chem.* 1992;96:4367–74.
  33. Kristof J, Frost RL, Felinger A, Mink J. FTIR spectroscopic study of intercalated kaolinite. *J Mol Struct.* 1997;410–411: 119–22.